nature genetics

A genome-wide scan identifies mutations in the gene encoding phosphodiesterase 11A4 (*PDE11A*) in individuals with adrenocortical hyperplasia

Anelia Horvath[1], Sosipatros Boikos[1], Christoforos Giatzakis[1], Audrey Robinson-White[1], Lionel Groussin[4], Kurt J Griffin[1,2], Erica Stein[1], Elizabeth Levine[1], Georgia Delimpasi[1], Hui Pin Hsiao[1], Meg Keil[2], Sarah Heyerdahl[1], Ludmila Matyakhina[1], Rossella Libè[4], Amato Fratticci[4], Lawrence S Kirschner[5], Kevin Cramer[6], Rolf C Gaillard[7], Xavier Bertagna[4], J Aidan Carney[3], Jérôme Bertherat[4], Ioannis Bossis[1] & Constantine A Stratakis[1,2]

Phosphodiesterases (PDEs) regulate cyclic nucleotide levels. Increased cyclic AMP (cAMP) signaling has been associated with *PRKAR1A* or *GNAS* mutations and leads to adrenocortical tumors and Cushing syndrome[1–7]. We investigated the genetic source of Cushing syndrome in individuals with adrenocortical hyperplasia that was not caused by known defects. We performed genome-wide SNP genotyping, including the adrenocortical tumor DNA. The region with the highest probability to harbor a susceptibility gene by loss of heterozygosity (LOH) and other analyses was 2q31–2q35. We identified mutations disrupting the expression of the PDE11A isoform-4 gene (*PDE11A*) in three kindreds. Tumor tissues showed 2q31–2q35 LOH, decreased protein expression and high cyclic nucleotide levels and cAMP-responsive element binding protein (CREB) phosphorylation. *PDE11A* codes for a dual-specificity PDE that is expressed in adrenal cortex and is partially inhibited by tadalafil and other PDE inhibitors[8,9]; its germline inactivation is associated with adrenocortical hyperplasia, suggesting another means by which dysregulation of cAMP signaling causes endocrine tumors.

Aberrant cAMP signaling has been linked to genetic forms of cortisol excess[1,2]. Somatic *GNAS* mutations are associated with macronodular adrenocortical hyperplasia in McCune-Albright syndrome (MAS)[2]. Micronodular adrenocortical hyperplasia and its pigmented variant, primary pigmented nodular adrenocortical disease (PPNAD) may be caused by germline inactivating mutations of the *PRKAR1A* gene[3–6]. Most affected individuals have PPNAD as a component of Carney complex (CNC), an autosomal dominant multiple neoplasia syndrome that is also caused mostly by *PRKAR1A* mutations[5].

Over the last several years, it has become apparent that there is more than one form of micronodular adrenocortical hyperplasia[7]. We identified a total of ten other individuals with Cushing syndrome and adrenocortical hyperplasia who did not have *PRKAR1A* mutations. In most of these individuals, the adrenal glands had an overall normal size and weight and featured multiple small yellow-to-dark brown nodules surrounded by a cortex with a uniform appearance (**Fig. 1a**). Microscopically, there was moderate diffuse cortical hyperplasia with mostly nonpigmented nodules, multiple capsular deficits and massive circumscribed and infiltrating extra-adrenal cortical excrescences with micronodules (**Fig. 1b**). Although overall there was no pigmentation by regular microscopy, electron microscopy did show granules of lipofuscin and features of a cortisol-producing adrenocortical hyperplasia (**Fig. 1c**). In other cases, the features of the disease were consistent with those of PPNAD caused by *PRKAR1A* mutations[1].

The mode of inheritance of this apparently genetic form of bilateral adrenocortical hyperplasia was uncertain: only one of the ten kindreds demonstrated clear inheritance from an affected mother to her affected daughter. All other individuals studied were the only affected individuals within their families. Preliminary studies using comparative genomic hybridization and BAC microarray hybridization of the tumor samples did not show any abnormalities (data not shown). We hypothesized that areas of the genome that are linked to the disease could be identified in a genome-wide scan: smaller-scale allelic losses

[1]Section on Endocrinology & Genetics, and [2]Pediatric Endocrinology Training Program, Developmental Endocrinology Branch, US National Institute of Child Health and Human Development, US National Institutes of Health, Bethesda, Maryland 20892, USA. [3]Department of Laboratory Medicine and Pathology, Mayo Clinic, Rochester, Minnesota 55905, USA. [4]Département Endocrinologie, Métabolisme & Cancer, Institut Cochin, Institut National de la Santé et de la Recherche Médicale (INSERM) U567 and Centre National de la Recherche Scientifique (CNRS) UMR 8104, and Centre de Référence des Maladies Rares de la Surrénale, Service d'Endocrinologie, Hôpital Cochin, Université Paris 5, Paris, 75679, France. [5]Divisions of Endocrinology and Human Cancer Genetics, Ohio State University, Columbus, Ohio 43210, USA. [6]Sapio Sciences, LLC, York, Pennsylvania 17402, USA. [7]Division d' Endocrinologie, Diabetologie et Metabolisme, Centre Hospitalier Universitaire Vaudois-CHUV, CH-1011 Lausanne, Switzerland. Correspondence should be addressed to C.A.S. (stratakc@mail.nih.gov).

Received 13 December 2005; accepted 26 April 2006; published online 11 June 2006; doi:10.1038/ng1809

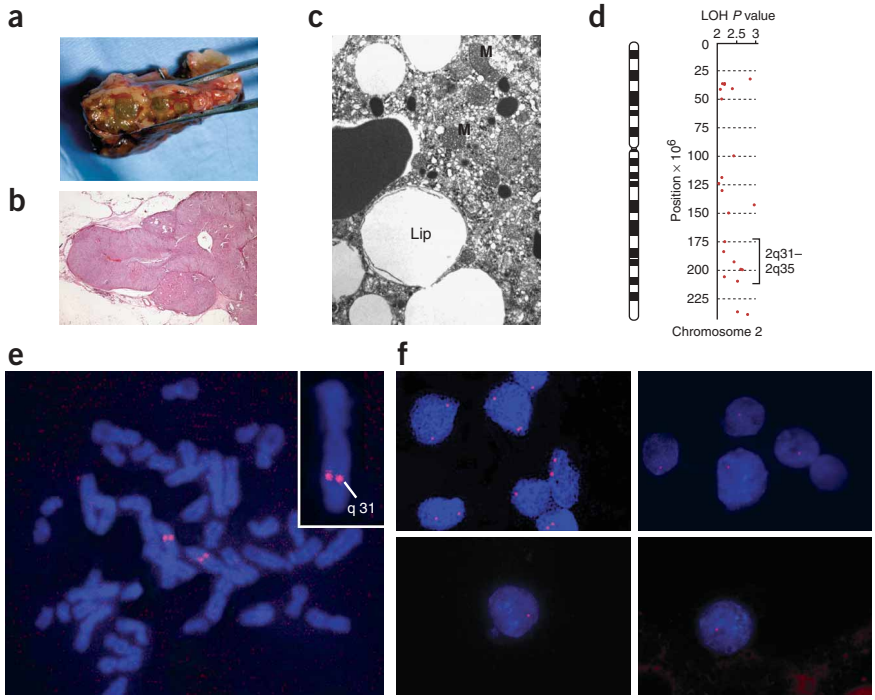

Figure 1 Micronodular BAH, identification of the 2q31–2q35 locus by LOH studies and *PDE11A* gene mapping and allelic losses. (**a**) Macroscopic appearance of an adrenal gland with micronodular adrenocortical hyperplasia. Multiple yellow-to-brown nodules are visible in the background of a normally shaped but hyperplastic gland. (**b**) Histological sections of the excised adrenal glands from individual CAR36.03 stained by hematoxylin and eosin (images obtained with a 1.25× lens). The normal adrenocortical zonation pattern is mildly disturbed, and intracapsular aggregates of cells and cortical excresenses in the periadrenal fat are prominent. (**c**) Electron microscopy showed granules of lipofuscin, lipid accumulation (Lip), giant mitochondria (M) and dilated smooth endoplasmic reticulum, all features of a cortisol-producing adrenal hyperplasia. (**d**) SNP analysis of the chromosome 2 identified a region with significant gene dosage changes in the distal q arm of chromosome 2, 2q31–2q35. (**e**) FISH with a probe containing the *PDE11A* gene (the RP11-428I14 BAC) on a metaphase spread from a normal human cell line mapped the *PDE11A* gene on the distal 2q (2q31.2) arm. (**f**) Upper left: FISH on tumor cells from one of the affected individuals shows the expected two signals per cell for a control probe from chromosome 6 (6q). Upper right, lower left and lower right: FISH on tumor cells from individuals with adrenocortical hyperplasia and *PDE11A* mutations showed allelic loss (one signal) of the RP11-428I14 BAC probe.

and gains could be identified by comparing tumor SNPs with those of the proband's peripheral DNA or that of his unaffected relatives. We genotyped ten tetrads of samples, each consisting of the two parents and the dyad of proband and tumor sample, using the Affymetrix 10K GeneChip. We analyzed LOH and other data by a number of different modules that were then evaluated by traditional statistics. We focused on regions coding for PDEs and other cAMP signaling genes. We then concentrated on region 2q31–2q35 because SNPs in this region were favored by all types of analyses, including LOH (**Supplementary Methods** online): several SNPs from 2q31–2q35 had shown LOH (**Fig. 1d**; **Supplementary Table 1** online), and, as a contiguous region, 2q31–2q35 was the largest in the LOH dataset.

There are two PDE genes in this chromosomal area: *PDE1A* on 2q32.1 and *PDE11A* on 2q31.2 (**Fig. 1e**). We included a SNP from within the *PDE11A* gene (*RS959157*) in the LOH analysis. One of its alleles was lost in all informative tumor samples from heterozygote affected individuals. We used FISH with a BAC probe that contains a large part of the 3′-region of the *PDE11A* gene; this hybridized to the 2q31.2 region (**Fig. 1e**) and showed losses in tumor cells from the adrenocortical specimens that were used in the genome-wide scan (**Fig. 1f**). PDE11A catalyzes the hydrolysis of both cAMP and cyclic GMP (cGMP) and is expressed in several endocrine tissues, including the adrenal cortex[8–11]. PDE1A is calmodulin dependent and hydrolyzes cGMP, primarily[12]; its SNP did not show consistent LOH (data not shown). *PDE11A* was an obvious candidate because of its location on the 2q31–2q35 region, its involvement in allelic losses and its known function and expression pattern.

The *PDE11A* locus, like that of other PDEs, has a complex genomic organization (**Fig. 2a**) that has recently been elucidated[13–17]. Of the four possible splice variants, only A4 is expressed in the adrenal cortex (**Fig. 2b**, left). PDE11A1 seems to be ubiquitous, whereas the PDE11A2 and PDE11A3 isoforms are expressed in testis[10,11,15,17]; among individuals with *PDE11A*-allelic losses, CAR14.03 had decreased mRNA without compensatory expression of other *PDE11A* isoforms (**Fig. 2b**, left). We also saw decreased protein expression in all tumor tissues (**Fig. 2b**, right). Immunohistochemistry (IHC) with a polyclonal antibody for PDE11A4 (ref. 11) showed homogeneous staining of the normal adrenal cortex (**Fig. 3a**,**b**) and decreased expression of this protein in the nodules of individuals with the disease (**Fig. 3c**,**d**).

We sequenced the *PDE11A* gene using primers amplifying all the known exons[17] (**Supplementary Table 2** online) in 16 individuals with adrenocortical hyperplasia and no *PRKAR1A* mutations: ten from the original cohort used in the genome-wide study, and six additional individuals with Cushing syndrome due to similar forms of hyperplasia. We identified five germline sequence variations in the heterozygote state: two frameshifts, one substitution that led to a premature stop codon (**Fig. 2c**) and two missense substitutions (**Supplementary Table 3** online). Two of the protein-truncating mutations were found in our original cohort of ten kindreds (in individuals CAR14.03 and CAR36.03); one more was found among the six additional subjects with adrenocortical hyperplasia and Cushing syndrome that were screened (in individual F12 (CAR950.03)) (**Table 1**, **Supplementary Table 3**).

The mutations disrupting the PDE11A4 protein expression were the two frameshifts (171delTfs41X and 1655_1657delTCT/insCCfs15X) and one base pair substitution (919C→T) (R307X) (**Fig. 2c**). Two more single–base pair substitutions, 2411G→A and 2599C→G, led to amino acid replacements (R804H and R867G, respectively) (**Supplementary Table 3**). We did not find any of the protein-truncating mutations of the *PDE11A* gene in a set of controls of mostly European descent, whereas we found both missense substitutions in them (**Supplementary Table 3**). We also found several other, benign polymorphisms (**Supplementary Table 4** online).

In one family (CAR14), the 919C→T (R307X) mutation was passed on from an affected mother to her affected daughter; both

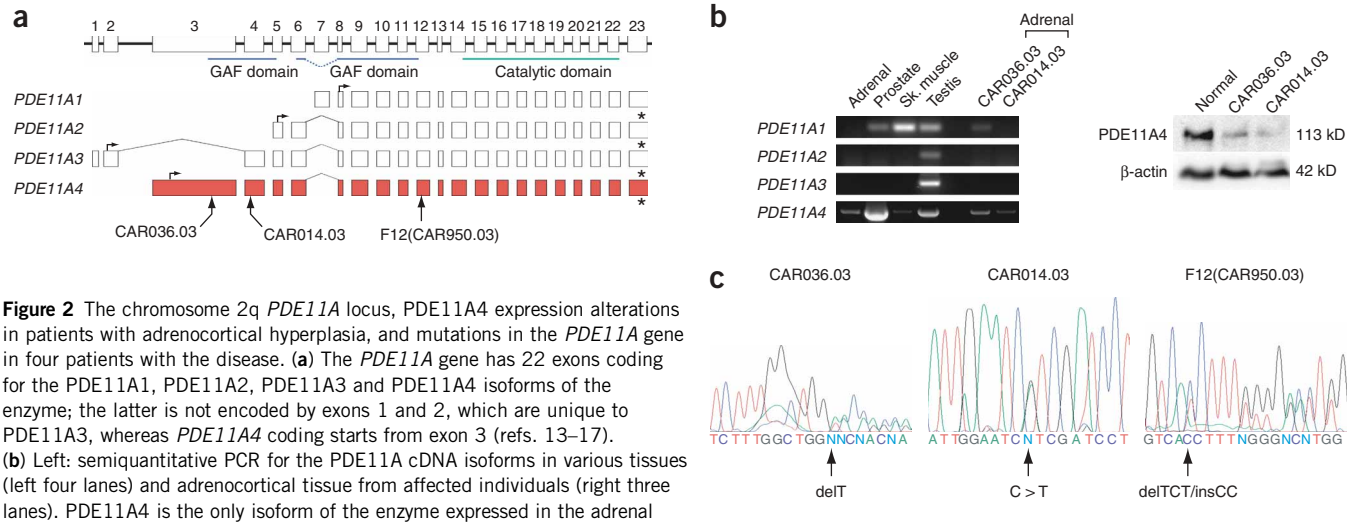

Figure 2 The chromosome 2q *PDE11A* locus, PDE11A4 expression alterations in patients with adrenocortical hyperplasia, and mutations in the *PDE11A* gene in four patients with the disease. (**a**) The *PDE11A* gene has 22 exons coding for the PDE11A1, PDE11A2, PDE11A3 and PDE11A4 isoforms of the enzyme; the latter is not encoded by exons 1 and 2, which are unique to PDE11A3, whereas *PDE11A4* coding starts from exon 3 (refs. 13–17). (**b**) Left: semiquantitative PCR for the PDE11A cDNA isoforms in various tissues (left four lanes) and adrenocortical tissue from affected individuals (right three lanes). PDE11A4 is the only isoform of the enzyme expressed in the adrenal gland, where it is expressed substantially less than in the prostate. PDE11A1 seems to be ubiquitous, whereas the PDE11A2 and PDE11A3 isoforms are expressed in testis[10,11,15,17]. At least one of the affected individuals with a *PDE11A*-inactivating mutation (CAR14.03) has decreased *PDE11A* mRNA in adrenal tissue but no compensating expression of any of the other isoforms. Right: protein blot of tissue lysates from normal adrenal cortex and from two of the affected individuals with *PDE11A* mutations showed decreased protein expression in all tumor tissues. (**c**) Mutations of the *PDE11A* gene in subjects CAR036.03, CAR014.03 and F12 (CAR590.03) (see also **Table 1** and **Supplementary Table 3**).

individuals had adrenocortical hyperplasia leading to Cushing syndrome, both underwent bilateral adrenalectomy and both of their tissues had classic pathological features of PPNAD. In the case of individual F12 (CAR950.03), we tested her healthy parents and found that they had the normal *PDE11A* sequence, indicating that the 1655_1657delTCT/insCCfs15X mutation developed *de novo* in the F12 kindred (**Supplementary Fig. 1** online). Individual CAR36.03 inherited her mutation, 171delTfs41X, from her father, CAR36.01 (**Supplementary Fig. 1**). The mother and an unaffected sibling of CAR36.03 carried the normal *PDE11A* sequence. Individual CAR36.01 had moderate adrenal enlargement and responded to the gradual administration of dexamethasone with the so-called 'paradoxical' rise of glucocorticoid secretion[5,7] (**Supplementary Fig. 1**).

The identification of *PDE11A* mutations and their familial inheritance allowed for the investigation of LOH by SNP or polymorphic marker studies. Two informative *PDE11A* SNPs on the mutation-bearing allele were retained by the tumor in the adrenocortical samples from CAR14.03 and CAR36.03 (**Supplementary Fig. 2** online). Segregation analysis of the *D2S1776* marker in the proximity of the *PDE11A* gene showed retention of the allele bearing the mutant gene by a tumor lysate sample in family CAR36 (**Supplementary Fig. 2**). SSCP analysis of another, microdissected specimen from this tumor showed homozygosity for the 171delT allele (data not shown).

cAMP and cGMP levels in tissue homogenates from affected individuals with *PDE11A* mutations were higher than those of control tissue samples (**Fig. 4a**,**b**). We also examined the effect of PDE11A4 defects on the phosphorylation status of CREB in tumors from the individuals with mutations and compared it with normal adrenal samples both by protein blotting and IHC. The ratio of phosphorylated (P)-CREB to CREB in the samples carrying mutant *PDE11A* was increased, as shown by protein blotting (**Fig. 4c**); a representative blot is shown in **Figure 4d**. The expression of CREB and P-CREB in normal adrenal tissues (data not shown) was significantly lower than in specimens with *PDE11A* mutations, as shown by IHC (**Figs. 4e–h**). Nuclear staining for P-CREB (**Figs. 4f**,**h**) was also greater than that for CREB (**Figs. 4e**,**g**) in tumors with mutations; staining for P-CREB was even further increased in nodular tissue compared with perinodular tissue.

These data are supportive of *PDE11A* being a gene associated with bilateral adrenocortical hyperplasia in the affected individuals studied here. The pathophysiological mechanism of the disease seems to be linked to increased cAMP levels, as in individuals with MAS[18], and the histopathological changes are similar to those in PPNAD, another disorder associated with increased cAMP signaling[2]. The frequency with which carriers of mutations in one of these genes present with

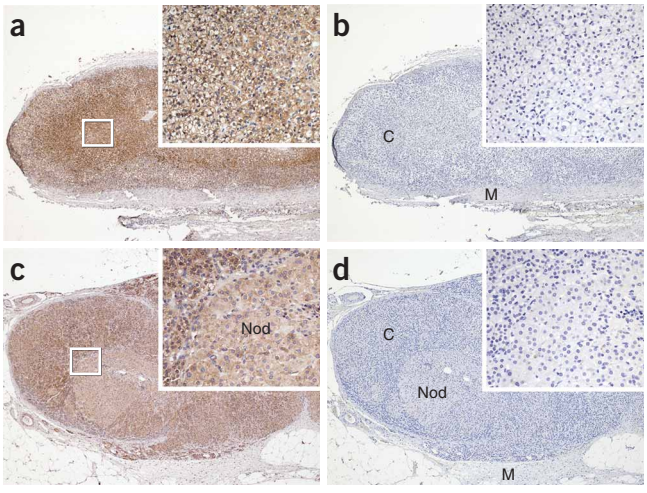

Figure 3 Immunohistochemistry of human adrenal glands using a polyclonal antibody to PDE11A reported in ref. 11. The larger image in each panel was taken with a 2.5× lens; insets were obtained with 40× magnification. (**a**) Normal adrenal cortex (C), but not medulla (M), expresses PDE11A homogenously. (**b**) Negative control staining of a consecutive section. (**c**) Decreased staining for PDE11A in a nodule (Nod) from the adrenal cortex of individual CAR36.03. The cortex (C) is otherwise mildly hyperplastic. (**d**) Negative control staining of a consecutive section.

Table 1 Individuals with Cushing syndrome and pathogenic *PDE11A* mutations

Individual	Age[a]	Clinical signs	Treatment	*PDE11A* mutation	Inheritance studies
CAR14.02	23	CS, ovarian cysts	BADX	919C→T (R307X)	AD
CAR14.03 (daughter of CAR14.02)	19	CS	BADX	919C→T (R307X)	AD
CAR36.03	7	CS, pancreatitis[b]	BADX	171delTfs41X	AD
F12 (CAR950.03)	37	CS	UADX	1655_1657delTCT/insCCfs15X	*De novo*

AD, autosomal dominant; BADX, bilateral adrenalectomy; CS, Cushing syndrome; UADX, unilateral adrenalectomy. [a]Age at the time of presentation. [b]This individual developed necrotizing pancreatitis shortly after her bilateral adrenalectomy; she succumbed to complications of this disease a month later.

classic Cushing syndrome seems to be higher in disease associated with *PRKAR1A* and *PDE11A* than in disease associated with *GNAS*, whereas the age at which Cushing syndrome presents in these disorders is exactly the reverse: *GNAS* mutation carriers present with Cushing syndrome almost always in infancy, whereas *PDE11A* or *PRKAR1A* mutation carriers present with Cushing syndrome in childhood and young adulthood. A number of factors (developmental, hormonal and perhaps gender-related) are likely to affect the expression of these mutations. The presence of allelic losses of the corresponding normal allele in adrenal tissues also seems to be a determining factor in the development of disease associated with *PRKAR1A* and *PDE11A* mutations, as both genes were identified using LOH studies[3].

PDE11A is the first PDE to be linked to an inherited condition associated with tumor formation. Defects in two other PDEs cause human genetic disorders: mutations in PDE6 subunits cause hereditary eye disease[19,20], whereas *PDE4B* abnormalities were recently linked to schizophrenia[21]. Additional PDEs have been associated with various mouse phenotypes, from infertility[22,23] to heart failure and arrhythmias[24]. Very little is known about PDE11A4 (refs. 10–12) or other PDEs in adrenal cortex, although adrenocortical tissue seems to show significant PDE activity in an *in vitro* model[25]. Indeed, our PDE11A expression studies in human adrenal cortex (**Figs. 2b** and **3a**) show that this enzyme is homogeneously expressed by the cortisol-producing zona fasciculata cells, along with a number of other PDEs (**Supplementary Fig. 3** online). In addition, PDE11A4 is strongly expressed in human prostate, at a level that is significantly higher than that in the adrenal gland (**Fig. 2b**). However, the single male with a mutation in the gene encoding PDE11A in this study (CAR36.01) was not known to have any significant prostatic pathology.

The activity of PDE11A is partially inhibited by tadalafil (Cialis) and weakly by sildenafil (Viagra)[8,9]. These medications are widely used for the treatment of erectile dysfunction, but searching the available drug toxicity databases, we could not identify any reports of adrenal malfunction or any other endocrine problems in affected individuals that have used these medications. A mouse model of *Pde11a* inactivation has been reported[26], and a role of this enzyme in spermatozoa physiology was suggested[26,27], but little else.

In conclusion, we have found inactivating mutations of *PDE11A* in a condition predisposing to the development of adrenocortical hyperplasia leading to Cushing syndrome. Genetic defects of the PDE genes have never before been linked to the development of any tumors. This discovery may shed light on some of the issues surrounding cAMP signaling and its involvement in tumorigenesis.

METHODS

Clinical studies and tissue samples. The institutional review boards of the US National Institute of Child Health and Human Development (NICHD), the US National Institutes of Health (NIH), the Mayo Clinic and Hospital Cochin (Paris, France) approved the contact of the families and the participation of their members in the NICHD protocols 95-CH-0059 and 00-CH-0160; informed written consent was obtained. Individuals with CNC or other forms of adrenocortical hyperplasia were classified as 'affected', as described previously[1,2,5,7]. Individuals who were diagnosed with Cushing syndrome (**Table 1**; **Supplementary Table 3**) by standard clinical testing and criteria underwent adrenalectomy. Blood and tissue samples were collected from affected individuals as previously described[7,28]. When possible, tissue was collected at surgery

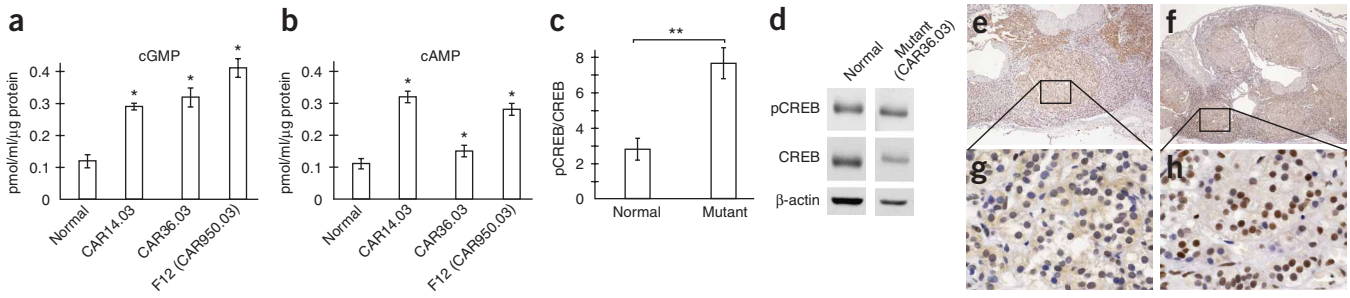

Figure 4 Effects of *PDE11A* mutations in cyclic nucleotide levels and CREB phosphorylation. (**a**) cGMP activity and (**b**) cAMP activity in adrenal tumors from affected individuals. Tissue lysates from three normal adrenal glands and those from CAR14.03, CAR36.03 and F12 (CAR950.03) were assayed separately for cAMP and cGMP content. All experiments were repeated at least twice, and each sample was run in triplicate. *, $P < 0.05$. (**c**) Tissue lysates from six normal adrenal glands and those from CAR14.03, CAR36.03 and F-12 (CAR950.03) ('Mutant') were tested by protein blotting using commercially available antibodies for CREB and P-CREB. The ratios were calculated after scanning the individual protein bands and correcting for β-actin optical density. The *y* axis measures random optical density units. **, $P < 0.001$. (**d**) Representative immunostaining for CREB and P-CREB from a normal adrenal specimen and one tumor bearing a mutant *PDE11A4* allele; these data are included in **a**. (**e**–**h**) Samples from normal adrenal glands (data not shown) and those from *PDE11A4* mutation–bearing tumors were stained using commercially available CREB and P-CREB antibodies. **e**–**h** show representative images from CAR14.03: staining for CREB (**e**) was less intense than that for P-CREB (**f**), especially within the nodular areas. A higher magnification of the nodular tissue is shown for CREB (**g**) and P-CREB (**h**) in the lower panels (60×), revealing intense, nuclear-specific staining.

and processed for routine histopathology and immunohistochemistry (IHC) after being formalin-fixed and paraffin-embedded; additional fragments were frozen immediately at –70 °C for later use. DNA was extracted from samples from all individuals, tissue samples and/or cell lines using standard methods (Qiagen). All adrenal samples were microdissected from their surrounding normal tissues from parts of the adrenal that would not normally include medullary or other tissues; thus, mostly abnormal tissue was used for DNA, mRNA and protein studies. All affected individuals have previously been screened for *PRKAR1A* mutations; tumor samples have been screened for *GNAS* mutations[7]. There were no coding sequence alterations in these genes (data not shown).

For light microscopy and immunocytochemistry, tissue was paraffin embedded; sections were then stained with hematoxylin and eosin (H&E) and synaptophysin, a marker for PPNAD and related adrenocortical tumors, as previously described[7]. All samples were also stained for PDE11A4, CREB and P-CREB (see below). For electron microscopy (**Fig. 1d**), tissue was obtained at the time of surgery and processed as previously described[7].

Genotyping and genome-wide scan for LOH. Complete details of all the analyses are available online (**Supplementary Methods**). Briefly, SNP genotyping was performed using the early-access Affymetrix Mapping 10K array according to the manufacturer's recommendations. Genotyping was performed at Genome Explorations. The raw data from the genotyping were downloaded to Microsoft Excel and exported to Sapio Sciences Exemplar software for various analyses. Given the small sample size and low statistical power (approximately eight cases, with two samples for each case from peripheral blood and tumors, and 16 parental controls), the objective was to use multiple methods of analysis to reduce the number of SNPs to be considered from ~11,000 to ~100. Contingency tables were then constructed on genotype and allele counts, providing multiple metrics for each SNP. Fisher's exact test and odds ratios were the primary statistics used. When calculating Fisher's by genotype, 1,200 SNP-genotype combinations had uncorrected $P < 0.05$. When calculating Fisher's by allele, 208 SNPs had uncorrected $P < 0.05$, and when calculating a P value for all SNPs based on a 2×3 table and using χ^2 analysis, 420 SNPs had uncorrected $P < 0.05$. Overall type I error rates were calculated retrospectively for each statistic using the Bonferroni method. Further analysis used Exemplar's genetic algorithm (GA) module to build models that are combinations of multiple loci via logical operators. Before feeding the input file to the GA, we used various feature selection methods, including statistical feature selection (Fisher's, cutoff of $P < 0.005$), as well as minor allele frequency variations between cases and controls (0.25–0.35 variance cutoff). After multiple GA runs producing several models with high classification accuracy (>95%), we combined the SNPs identified by the above statistics (top 50 from each metric) and the GA to produce a final list for consideration. We removed any duplicates and one of any two neighboring SNPs that were in perfect linkage disequilibrium. We performed LOH analysis to detect possible deletions in the chromosomes: A P value was calculated for each SNP; over ~200 had $P < 0.05$ (the chromosome 2 SNPs and their P values are listed in **Supplementary Table 1**). From this analysis, we found agreement with several loci, including, most importantly, the 2q31–2q35 region identified by the other methods. **Figure 1d** shows significant LOH for chromosome 2 SNPs and the location of the *PDE11A* gene region.

Identification of a BAC containing the *PDE11A* gene and FISH on tumor cells. The RP11-428I14 BAC, which contains a large part of the *PDE11A* gene, was identified in Ensembl. This 183436 bp-long BAC contains the 3′-part of the *PDE11A* gene that is shared by all isoforms (A1, A2, A3 and A4) and is flanked by the centromeric *D2S2173* and the telomeric *D2S2757* markers. This and other BACs were obtained from the BAC-PAC Resource Center, grown and screened as we described previously[28]. The RP11-428I14 BAC was screened using primers amplifying exon 15 of the *PDE11A* gene (data not shown). The probe mapped to chromosomal region 2q31.2 (**Fig. 1e**). Touch preparations on sialinized slides were prepared from frozen tumor samples that were carefully microdissected from normal tissue and kept at –20 °C until hybridization.

FISH was performed using the RP11-428I14 BAC and other BACs containing control loci (such as one on chromosomes 6q and 2p12–2p16 and the 17q22-24 *PRKAR1A* locus) and the α-satellite probe for identification of chromosome 2 (Vysis), as we have described elsewhere[28]. Probes were then labeled with digoxigenin-11–labeled dUTP (Roche Molecular Biochemicals) by nick-translation and hybridized to the touch preparations of the tumor samples. After hybridization, cells were counterstained with 4′,6′-diamidino-2-phenylindol-dihydrochloride (DAPI). Hybridization signals were analyzed with the use of a Leica epifluorescence microscope, and fluorescence images were automatically captured on a Photometrics cooled-CCD camera using IP Lab Image software (Scanalytics). We scored 200 interphases with strong hybridization signals. The presence of >25% cells with only one signal was interpreted as indicative of an allelic deletion (**Fig. 1f**).

***PDE11A* gene structure, primers, LOH, sequencing, and other genetic screening.** The genomic sequence of human *PDE11A* was used to design intronic primers to amplify all exons and exon/intron junctions, as provided in ref. 17. Our primer sequences are listed in **Supplementary Table 2**. PCR was performed in 50 µl of a solution containing 10 mM Tris-HCl (pH 8.3), 50 mM KCl, 2 mM $MgCl_2$, 0.2 mM dNTP, 0.5 pmol of each primer, 50 ng genomic DNA and 2.5 units of *Taq* DNA polymerase. The reaction consisted of 25 cycles of denaturation at 94 °C for 30 s, annealing at the indicated temperature for 40 s and extension at 72 °C for 30 s. The products were gel purified and sequenced on an ABI PRISM 3730 automated DNA sequencer (Applied Biosystems). Sequences were analyzed using Vector NTI Advance (Invitrogen). Amplicons with sequence changes were subjected to TOPO-TA cloning (Invitrogen); plasmids were then sequenced by standard methods. The presence of all sequence alterations was confirmed at least twice by both forward and reverse sequencing or restriction enzyme digestion (see below). Control samples from ethnically matched samples were investigated as listed in **Supplementary Table 3**. The Coriel Institute collection of control samples of mostly European descent was also used and sequenced at Polymorphic DNA Technologies or screened by *Bsp*H1 digestion (see below) at GeneDx.

The *PDE11A* locus was also checked for major deletions and other genomic rearrangements by DNA blotting in specimens that were negative for *PDE11A* mutations (data not shown). Details of the probes and their sequences are available upon request. There were no major alterations detected in any samples. Finally, restriction analysis was used for the verification of mutations that altered restriction enzyme sites. To detect the 2411G→A substitution, which creates a *Bsp*HI restriction site, endonuclease digestion was performed according to the manufacturer's instructions (New England Biolabs). In brief, 200 ng purified PCR product (QiaQuick; Qiagen) was digested with 5 units *BspHI* for 2 h at 37 °C in a total reaction volume of 20 µl. The restriction products were analyzed on 2% (wt/vol) agarose gel.

After identifying the allele bearing the mutation by sequencing or phase analysis, we performed LOH analysis of two SNPs from within the *PDE11A* gene that were informative (RSid1435572 and RSid1997207) using data from the Affymetrix 10K GeneChip. Comparison of the intensities of the peripheral and tumor DNA signals obtained at Genome Explorations was done as recently described[29] (**Supplementary Figs. 2** and **3**). We sought confirmation for these samples in cases where enough tissue was available by studying neighboring microsatellite markers: for kindred CAR36, marker *D2S1776* was informative (**Supplementary Fig. 2**). We analyzed this tetranucleotide repeat on a gel by standard methods and publicly available PCR conditions and primers. Because this analysis showed some 'contamination' of the tumor tissue with normal cells, SSCP analysis and linear PCR amplification using [γ-^{32}P]dATP-labeled primer on minute amounts of DNA from nodular and perinodular tissue showed homozygosity and heterozygosity, respectively (data not shown).

mRNA, protein studies, immunohistochemistry and cAMP and cGMP assays. Tissues and cell lines from individuals and their tumors were maintained in RPMI-1640 or DMEM supplemented with 10–15% fetal bovine serum. Total cellular protein extracts from frozen tissues or cultured cells were prepared using RIPA buffer (20 mM HEPES, 250 mM NaCl, 10% glycerol, 1% NP-40, 0.5% deoxycholate, 2 mM DTT and protease inhibitor) (**Figs. 2b** and **4b**). We analyzed 20 µg from cell lysates (and 50 µg from tissue lysates) of total protein by SDS/PAGE using a 4–20% gradient gel. The proteins were transferred to nitrocellulose membranes, and PDE11A4 was detected using a rabbit polyclonal antibody specific for PDE11A as directed by the manufacturer, Abcam (ab14624), at 1:500 (**Fig. 2b**) and 1:1,000 (**Fig. 3**) dilutions, as described previously[11]. The same antibody was used for

immunohistochemistry of paraffin-embedded tissue slides (**Fig. 3**). Similar methods were used for the CREB and P-CREB immunostaining (protein blot and IHC); all mutant tissues were used in these experiments (**Fig. 4**). The antibodies are commercially available from Upstate.

Normal adrenal, prostate, skeletal muscle and testicular mRNA was obtained from Ambion and was reverse transcribed into cDNA using the First-Strand cDNA Synthesis Kit (Invitrogen). PCR primer sequences were designed using VectorNTI software (Informax) to amplify the 5′-regions of PDE11A1, PDE11A2, PDE11A3 and PDE11A4 isoform-specific full-length cDNA using Accuprime *Taq* High-Fidelity Polymerase (Invitrogen) (**Fig. 2b**). Similarly, primers were designed as published elsewhere[30] to check for the expression of other PDEs in adrenal cortex (**Supplementary Fig. 3**). All primers, including those for the other PDE cDNA, are given in **Supplementary Table 2**.

Quantitative determination of cAMP and cGMP levels in cell lysates from tissue samples (**Fig. 4**) was done using commercially available assays; the kits were obtained from R&D Systems. Both assays are based on competitive binding, in which endogenous cAMP or cGMP levels compete with a fixed amount of alkaline phosphatase–labeled cyclic nucleotides; the assays are colorimetric and absorbance is read at 405 nm.

Accession codes. Ensembl: *PDE11A* (genomic sequence), ENSG00000128655. GenBank: *PDE11A1* (cDNA), AJ251509.1; *PDE11A2* (cDNA), AF281865.1; *PDE11A3* (cDNA), AB038041.1; *PDE11A4* (cDNA), NM_016953.2; *PDE1A* (cDNA), NM_005019; *PDE4A* (cDNA), NM_006202; *PDE4B* (cDNA), NM_002600; *PDE4C* (cDNA), NM_000923; *PDE4D* (cDNA), NM_006203; *PDE7A* (cDNA), NM_002603; *PDE8A* (cDNA), NM_003719; *PDE9A* (cDNA), NM_002606;

URLs. Genome Explorations: http://www.genome-explorations.com; Sapio Sciences: http://www.sapiosciences.com. The RP11-428I14 BAC was identified at http://www.ensembl.org/Homo_sapiens/contigview?l=2:178318319-178798573. Coriell Institute for Medical Research: http://ccr.coriell.org/ccr/; Polymorphic DNA Technologies: http://www.polymorphicdna.com/. Screening by *Bsp*H1 digestion: http://www.genedx.com. Information on *PDE11A*, its structure and mRNA was obtained at http://www.gdb.org. Protocol for SSCP analysis can be found at http://www.uga.edu/srel/DNA_Lab/SSCP'96V2.rtf.

Note: Supplementary information is available on the Nature Genetics website.

ACKNOWLEDGMENTS

This work is dedicated to our patients and their families. It was supported by US NIH intramural project Z01-HD-000642-04 to C.A.S. and, in part, by Groupement d'Intérêt Scientifique-Institut National de la Santé et de la Recherche Médicale Institut des Maladies Rares and the Plan Hospitalier de Recherche Clinique (AOM 02068) to the Comete Network. We thank S. Libutti and R. Alexander (National Cancer Institute (NCI), NIH) for expert surgical care on the individuals described in this study. We thank the nursing and other support staff of NICHD, NIH on the former 8W and 9W, and current 1NW and 5NW wards of the National Institutes of Health Warren Grant Magnuson Clinical Center for their support of our research studies and their help in the management of patients with adrenal tumors. We also thank D. Gunther (University of Washington, Seattle) and W.W. de Herder (Department of Internal Medicine, Endocrinology, Erasmus Medical Center, Rotterdam, the Netherlands) and the many other clinicians who have sent us samples from their patients. DNA samples from France were screened in that country for *PRKAR1A* mutations by E. Clauser, Unité d'Oncogénétique, CHU Cochin, Paris, and by E. Jullian, Institut Cochin, INSERM U567, Paris, to whom we are grateful. We thank C. Wayman (Discovery Biology, Pfizer Global Research and Development, Sandwich, Kent, UK) and J. Beavo (Department of Pharmacology, University of Washington, Seattle) for insightful advice in the field of PDE11A and their collaboration on the *Pde11a*$^{-/-}$ mouse. We thank I. Aksentijevich and E. Remmers (National Institute of Arthritis and Musculoskeletal and Skin Diseases, NIH), B. Brooks (National Eye Institute, NIH) and F. Porter (NICHD, NIH) for providing us with control DNA samples; K. Calis and F. Pucino (Pharmacy Department, NIH Clinical Center) for checking the PDE inhibitors toxicity database; and M. Abu-Asab and M. Tsokos (Laboratory of Pathology, NCI, NIH) for expert assistance with electron miscroscopy of adrenocortical specimens. We also thank V. Manganiello (National Heart, Lung and Blood Institute, NIH) and A. Spiegel (National Institute of Diabetes and Digestive and Kidney Diseases, NIH) for discussions on phosphodiesterases and cAMP signaling. We thank W.-Y. Chan's laboratory and staff (NICHD, NIH) for accommodating our increased sequencing needs and P. Soni for assisting with sequencing analysis. Finally, we thank C.A. Bondy and O.M. Rennert (NICHD, NIH) for editing our manuscript and for their continuing support of our studies.

AUTHOR CONTRIBUTIONS

C.A.S.: overall design and planning of the project, clinical evaluation of patients, analysis of the genome-wide genotyping, selection of *PDE11A4* as a candidate gene, overall supervision and organization of experiments, presentation of results, design of figures and writing the manuscript. C.A.S., J.A.C. and J.B. are principal investigators in the International Carney Complex Consortium. C.A.S. is a Senior Investigator at NICHD, which provided most of the funding for this project under an intramural NIH grant to C.A.S. A.H.: participation in specimen collection, database construction, analysis of the genome-wide genotyping, selection of candidate genes, design and optimization of the amplification and sequencing protocols, sequencing analysis, identification of pathogenic and polymorphic genetic variations, participation in organization of working processes, participation in the presentation of the results and editing of the paper. S.B.: participation in specimen collection, database construction sequencing analysis, FISH analysis; PDE11A4 protein expression evaluation (protein blot analysis, immunohistochemistry). C.G.: participation in the design of the project, expression of the *PDE11A* isoforms in different tissues, *in vitro* functional analysis of the effect of the pathogenic genetic variants, participation in the analysis of the cAMP and cGMP activity data, analysis for LOH (SSCP and microsatellite analysis), participation in the presentation of the results and editing of the paper. A.R.-W.: *in vitro* cAMP and cGMP assays and production of other functional data. L.G.: sequencing analysis and specimen collection; co-investigator in the consortium. K.J.G.: PDE11A4 expression analysis, mouse tissue analysis, editing the paper. E.S.: PDE11A4 expression analysis and *in vitro* assays. E.L., G.D. and H.P.H.: sequencing analysis. M.K.: clinical specimen collection and evaluation of patients. S.H: PDE11A4 expression analysis (protein blots, cDNA, mRNA). L.M.: FISH analysis of adrenocortical tumor specimens. R.L. and A.F.: sequencing analysis. L.S.K.: clinical specimen collection, mouse data analysis, editing the manuscript. K.C.: genome-wide genotyping, statistical evaluation of the data. R.C.G.: clinical specimen collection, patient evaluation. X.B.: clinical specimen collection, patient evaluation; co-investigator in the consortium. J.A.C.: design and planning of the project, clinical specimen collection, patient evaluation, review of all histopathology, editing of the manuscript. J.B.: design and planning of the project,, clinical specimen collection, patient evaluation, editing of the manuscript. I.B.: *in vitro* functional analysis of the effect of the pathogenic genetic variants, analysis of the cAMP and cGMP activity data, analysis for LOH (SSCP and microsatellite analysis), PDE11A protein expression evaluation (protein blot analysis), participation in the organization of most experiments and the presentation of results, editing of the manuscript.

COMPETING INTERESTS STATEMENT

The authors declare competing financial interests (see the *Nature Genetics* website for details).

Published online at http://www.nature.com/naturegenetics
Reprints and permissions information is available online at http://npg.nature.com/reprintsandpermissions/

1. Stratakis, C.A. & Kirschner, L.S. Clinical and genetic analysis of primary bilateral adrenal diseases (micro- and macronodular disease) leading to Cushing syndrome. *Horm. Metab. Res.* **30**, 456–463 (1998).
2. Bourdeau, I. & Stratakis, C.A. Cyclic AMP-dependent signaling aberrations in macronodular adrenal disease. *Ann. NY Acad. Sci.* **968**, 240–255 (2002).
3. Kirschner, L.S. *et al.* Mutations of the gene encoding the protein kinase A type I-alpha regulatory subunit in patients with the Carney complex. *Nat. Genet.* **26**, 89–92 (2000).
4. Kirschner, L.S., Sandrini, F., Monbo, J., Lin, J.P., Carney, J.A. & Stratakis,, CA. Genetic heterogeneity and spectrum of mutations of the *PRKAR1A* gene in patients with the Carney complex. *Hum. Mol. Genet.* **9**, 3037–3046 (2000).
5. Stratakis, C.A., Kirschner, L.S. & Carney, J.A. Clinical and molecular features of the Carney complex: diagnostic criteria and recommendations for patient evaluation. *J. Clin. Endocrinol. Metab.* **86**, 4041–4046 (2001).
6. Groussin, L. *et al.* Mutations of the PRKAR1A gene in Cushing's syndrome due to sporadic primary pigmented nodular adrenocortical disease. *J. Clin. Endocrinol. Metab.* **87**, 4324–4329 (2002).
7. Gunther, D.F. *et al.* Cyclical Cushing syndrome presenting in infancy: an early form of primary pigmented nodular adrenocortical disease, or a new entity? *J. Clin. Endocrinol. Metab.* **89**, 3173–3182 (2004).
8. Saenz de Tejada, I., Argulo Frutos, J., Gadau, M. & Florio, V. Comparative selectivity profiles of tadalafil, sildenafil and vardenafil using an in vitro phosphodiesterase acticity assay. *Int. J. Impot. Res.* **14** (Suppl.), S20 (2002).

9. Gbekor, E. *et al.* Phosphodiesterase 5 inhibitor profiles against all human phosphodiesterase families: implications for use as pharmacological tools. *J. Urol.* **167** (Suppl.), 246 (2002).
10. Loughney, K., Taylor, J. & Florio, V.A. 3′, 5′-cyclic nucleotide phosphodiesterase 11A: localization in human tissues. *Int. J. Impot. Res.* **17**, 320–325 (2005).
11. D'Andrea, M.R. *et al.* Expression of PDE11A in normal and malignant human tissues. *J. Histochem. Cytochem.* **53**, 895–903 (2005).
12. Michibata, H., Yanaka, N., Kanoh, Y., Okumura, K. & Omori, K. Human Ca2+/calmodulin-dependent phosphodiesterase PDE1A: novel splice variants, their specific expression, genomic organization, and chromosomal localization. *Biochim. Biophys. Acta* **1517**, 278–287 (2001).
13. Hetman, J.M. *et al.* Cloning and characterization of two splice variants of human phosphodiesterase 11A. *Proc. Natl. Acad. Sci. USA* **97**, 12891–12895 (2000).
14. Fawcett, L. *et al.* Molecular cloning and characterization of a distinct human phosphodiesterase gene family: PDE11A. *Proc. Natl. Acad. Sci. USA* **97**, 3702–3707 (2000).
15. Yuasa, K. *et al.* Isolation and characterization of two novel phosphodiesterase PDE11A variants showing unique structure and tissue-specific expression. *J. Biol. Chem.* **275**, 31469–31479 (2000).
16. Yuasa, K., Ohgaru, T., Asahina, M. & Omori, K. Identification of rat cyclic nucleotide phosphodiesterase 11A (PDE11A): comparison of rat and human PDE11A splicing variants. *Eur. J. Biochem.* **268**, 4440–4448 (2001).
17. Yuasa, K., Kanoh, Y., Okumura, K. & Omori, K. Genomic organization of the human phosphodiesterase PDE11A gene. Evolutionary relatedness with other PDEs containing GAF domains. *Eur. J. Biochem.* **268**, 168–178 (2001).
18. Weinstein, L.S. *et al.* Activating mutations of the stimulatory G protein in the McCune-Albright syndrome. *N. Engl. J. Med.* **325**, 1688–1695 (1991).
19. Gal, A., Orth, U., Baehr, W., Schwinger, E. & Rosenberg, T. Heterozygous missense mutation in the rod cGMP phosphodiesterase beta-subunit gene in autosomal dominant stationary night blindness. *Nat. Genet.* **7**, 64–68 (1994).
20. Huang, S.H. *et al.* Autosomal recessive retinitis pigmentosa caused by mutations in the alpha subunit of rod cGMP phosphodiesterase. *Nat. Genet.* **11**, 468–471 (1995).
21. Millar, J.K. *et al.* DISC1 and PDE4B are interacting genetic factors in schizophrenia that regulate cAMP signaling. *Science* **310**, 1187–1191 (2005).
22. Jin, S.L., Richard, F.J., Kuo, W.P., D'Ercole, A.J. & Conti, M. Impaired growth and fertility of cAMP-specific phosphodiesterase PDE4D-deficient mice. *Proc. Natl. Acad. Sci. USA* **96**, 11998–12003 (1999).
23. Masciarelli, S. *et al.* Cyclic nucleotide phosphodiesterase 3A-deficient mice as a model of female infertility. *J. Clin. Invest.* **114**, 196–205 (2004).
24. Lehnart, S.E. *et al.* Phosphodiesterase 4D deficiency in the ryanodine-receptor complex promotes heart failure and arrhythmias. *Cell* **123**, 25–35 (2005).
25. Kawamura, M., Kagata, M., Masaki, E. & Nishi, H. Phyllodulcin, a constituent of 'Amacha', inhibits phosphodiesterase in bovine adrenocortical cells. *Pharmacol. Toxicol.* **90**, 106–108 (2002).
26. Wayman, C. *et al.* Phosphodiesterase 11 (PDE11) regulation of spermatozoa physiology. *Int. J. Impot. Res.* **17**, 216–223 (2005).
27. Francis, S.H. Phosphodiesterase 11 (PDE11): is it a player in human testicular function? *Int. J. Impot. Res.* **17**, 467–468 (2005).
28. Bertherat, J. *et al.* Molecular and functional analysis of *PRKAR1A* and its locus (17q22–24) in sporadic adrenocortical tumors: 17q losses, somatic mutations, and protein kinase A expression and activity. *Cancer Res.* **63**, 5308–5319 (2003).
29. Ting, J.C., Ye, Y., Thomas, G.H., Ruczinski, I. & Pevsner, J. Analysis and visualization of chromosomal abnormalities in SNP data with SNPscan. *BMC Bioinformatics* **7**, 25 (2006).
30. Persani, L. *et al.* Induction of specific phosphodiesterase isoforms by constitutive activation of the cAMP pathway in autonomous thyroid adenomas. *J. Clin. Endocrinol. Metab.* **85**, 2872–2878 (2000).